



DARPinS Recognizing the Tumor-Associated Antigen EpCAM Selected by Phage and Ribosome Display and Engineered for Multivalency

Nikolas Stefan^{1†}, Patricia Martin-Killias^{1†}, Sascha Wyss-Stoeckle¹, Annemarie Honegger¹, Uwe Zangemeister-Wittke^{1,2} and Andreas Plückthun^{1*}

¹Department of Biochemistry, University of Zürich, Winterthurerstrasse 190, 8057 Zurich, Switzerland

²Institute of Pharmacology, University of Bern, Friedbühlstrasse 49, CH-3010 Bern, Switzerland

Received 7 August 2011;
accepted 8 September 2011
Available online
21 September 2011

Edited by F. Schmid

Keywords:

Designed Ankyrin Repeat Proteins (DARPinS); epithelial cell adhesion molecule (EpCAM); phage display; ribosome display; tumor targeting

Designed Ankyrin Repeat Proteins (DARPinS) represent a novel class of binding molecules. Their favorable biophysical properties such as high affinity, stability and expression yields make them ideal candidates for tumor targeting. Here, we describe the selection of DARPinS specific for the tumor-associated antigen epithelial cell adhesion molecule (EpCAM), an approved therapeutic target on solid tumors. We selected DARPinS from combinatorial libraries by both phage display and ribosome display and compared their binding on tumor cells. By further rounds of random mutagenesis and ribosome display selection, binders with picomolar affinity were obtained that were entirely monomeric and could be expressed at high yields in the cytoplasm of *Escherichia coli*. One of the binders, denoted Ec1, bound to EpCAM with picomolar affinity ($K_d=68$ pM), and another selected DARPin (Ac2) recognized a different epitope on EpCAM. Through the use of a variety of bivalent and tetravalent arrangements with these DARPinS, the off-rate on cells was further improved by up to 47-fold. All EpCAM-specific DARPinS were efficiently internalized by receptor-mediated endocytosis, which is essential for intracellular delivery of anticancer agents to tumor cells. Thus, using EpCAM as a target, we provide evidence that DARPinS can be conveniently selected and rationally engineered to high-affinity binders of various formats for tumor targeting.

© 2011 Elsevier Ltd. All rights reserved.

Introduction

Specific recognition of tumor-associated antigens is a key requirement for ligand-targeted diagnostics and cancer therapeutics. To date, antibodies and antibody fragments are the most widely used class of proteins for tumor targeting with imaging reagents or therapeutic agents. Despite recent progress in the field, however, cure rates for solid tumors are still low, and the efficacy of targeted drug delivery must be increased. One possibility is to design new targeting ligands that can be readily engineered into cancer therapeutics with improved pharmacologic properties and efficacy.

*Corresponding author. E-mail address:

plueckthun@bioc.uzh.ch.

† N.S. and P.M.-K. contributed equally to this work.

Abbreviations used: DARPin, Designed Ankyrin Repeat Protein; EpCAM, epithelial cell adhesion molecule; SRP, signal recognition particle; IMAC, immobilized metal affinity chromatography; sfGFP, superfolder green fluorescent protein; FITC, fluorescein isothiocyanate; MFI, mean fluorescence intensity; SPR, surface plasmon resonance; siRNA, small interfering RNA; DMEM, Dulbecco's modified Eagle's medium; PBS, phosphate-buffered saline; BSA, bovine serum albumin; EDTA, ethylenediaminetetraacetic acid; HA, hemagglutinin.

Previously, we described combinatorial libraries of recombinant modular proteins, termed “Designed Ankyrin Repeat Proteins” (DARPinS), which are well suited for this purpose, as they show favorable biophysical properties, such as high expression yield and low aggregation tendency.^{1–4} DARPinS are built from consecutive 33-amino-acid repeats, each forming a β -turn followed by two antiparallel α -helices. Internal repeat modules, in which seven residues were randomized, are flanked by constant capping repeats that shield the hydrophobic core, generating a small protein of 14–21 kDa with a randomized binding surface. Recently, the C-terminal capping repeat was redesigned to further improve the stability of these proteins.^{5,6} Their stable and yet adaptable structure, including the possibility to create hetero-oligomers of various geometries, small molecular weight and ease of production make them suitable tools for biomedical applications. Moreover, the introduction of unique cysteines allows site-specific modification and conjugation with various effector moieties.

We isolated several high-affinity binders against various targets from DARPin libraries mostly by ribosome display.^{2–4} Ribosome display is performed entirely *in vitro*^{7,8} and in combination with error-prone PCR constitutes an ideal tool for affinity maturation of binding proteins, since mutations can be easily introduced after each selection round.⁹ Phage display was also used to select DARPinS from libraries, but the standard filamentous phage system had to be modified for the display of these proteins, which fold rapidly already in the cytoplasm of the phage-producing *Escherichia coli*. Through the use of a signal recognition particle (SRP)-dependent signal sequence,¹⁰ co-translational transport is achieved, and such a DARPin phage library was successfully used to efficiently select binders against a wide range of targets.¹¹

We recently reported on DARPinS recognizing Her2 (human epidermal growth factor receptor 2) overexpressed in various carcinomas.^{3,8,12} Another attractive target on solid tumors is the epithelial cell adhesion molecule (EpCAM), which has repeatedly been shown to fulfill the requirements of a selective tumor marker, including the fraction of tumor-initiating cells.^{13,14} EpCAM is expressed in solid tumors with high homogeneity and is well internalized, thereby promoting the intracellular delivery of destructive payloads.^{15,16} EpCAM was initially described as a homophilic cell–cell adhesion molecule of 39–42 kDa, consisting of an extracellular part with an epidermal growth factor-like domain and a human thyroglobulin-like domain, a single trans-membrane helix and a short cytoplasmic tail.¹⁷ More recent studies demonstrated its role as an oncogenic signaling molecule activated via regulated intra-membrane proteolysis, resulting in the liberation of the cytoplasmic domain, which then associates with

components of the *wnt* pathway and induces transcription of *c-myc* and cyclins.^{18,19}

Screening of a broad range of target epitopes is initially useful, since binding proteins employed for tumor targeting must fulfill a number of requirements. In this study, it was therefore of interest to select EpCAM-specific DARPinS using ribosome display and phage display in parallel. Indeed, we obtained different binders by both methods, which we can partially rationalize by the experimental setup of both methods. Recently, we reported application data from a first generation of EpCAM-specific binders and demonstrated their promise for tumor targeting and drug delivery.¹⁵ The aim of the present study was to examine the details of the selection process and characterize EpCAM binders in more detail in order to obtain and further engineer binders with further improved biophysical properties to make tumor targeting even more efficient. We could by subsequent evolutionary rounds of ribosome display not only obtain binders with affinities in the picomolar range but also improve the properties of the evolved binders to prevent self-dimerization. The DARPinS were analyzed for cell binding and internalization to assess their potential for intracellular delivery of cytotoxic agents. In addition, multivalent fusion proteins consisting of up to four DARPinS recognizing EpCAM were engineered in various geometries. We demonstrate that some of these constructs dissociate from EpCAM-positive tumor cells almost 50-fold more slowly than the high-affinity monovalent DARPinS from which they were assembled, resulting in immeasurably slow dissociation rates from cells.

Results

Selection of EpCAM-specific DARPinS using SRP phage display

To increase the possibility of obtaining binders against different EpCAM epitopes, we selected DARPinS with both SRP phage display^{10,11} and ribosome display.^{8,9,20} For both procedures, the biotinylated extracellular domain of human EpCAM (bEpEx) was used as target. Three rounds of SRP phage selection were performed with bEpEx immobilized to, alternately, neutravidin or streptavidin bound to a solid plastic surface. The phage display DARPin library was in the N3C format. Specific EpCAM enrichment was already observed in the second round (Supplementary Fig. 1a), but it was notably stronger after the third round. Individual DARPinS selected in the third round were screened for specific EpCAM binding by crude extract ELISA. DNA sequencing of 20 clones revealed one dominant clone, named EPH1, which

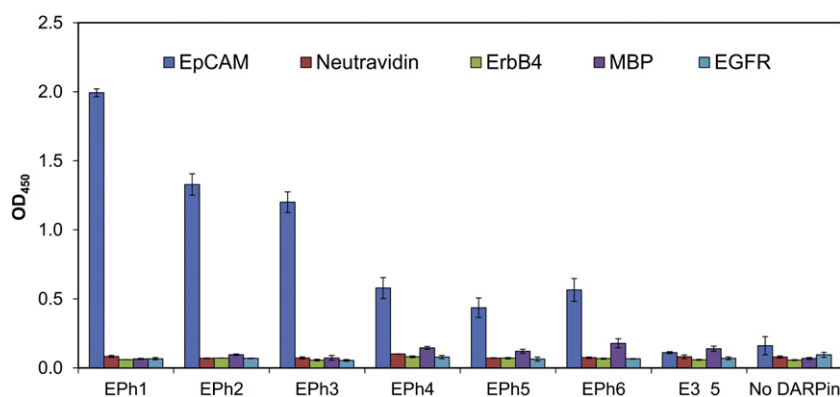


Fig. 1. Binding specificities of selected DARPins. The six DARPins selected by phage display were purified and tested in ELISA for binding to EpCAM, neutravidin, ErbB4, maltose binding protein (MBP) and epidermal growth factor receptor (EGFR). As further controls, an unselected member of the library (E3_5) and the background binding of the detection antibodies are shown in the absence of any DARPIn (No DARPIn).

contained a deletion of two amino acids between the N-terminal capping repeat and the first internal repeat (see below). The deletion seemed to be important for EpCAM binding, since mutants in which the deletion was corrected showed reduced affinity to EpCAM when tested by ELISA (data not shown).

Epitope masking

To increase the diversity and select DARPins binding to different EpCAM epitopes, we used an epitope masking strategy.²¹ The dominant binder obtained by the initial selection step, EPh1, was expressed, purified and added to new selection rounds in 100-fold excess to block the dominant epitope and force the selection to other epitopes. Since immobilization of the antigen can mask potential binding epitopes, the new selection rounds were performed in solution. The output from the first selection round on target immobilized on surface-coated streptavidin formed the starting material for another four rounds of panning in solution (with biotinylated EpCAM subsequently immobilized on streptavidin-coated magnetic beads). When analyzed by phage ELISA, output phages from rounds 3 em and 4 em (em: epitope masking) showed EpCAM binding in the presence and absence of the dominant binder EPh1 (Supplementary Fig. 1b), suggesting that some of the newly selected DARPins recognized different epitopes than EPh1. Individual DARPins from round 4 em were analyzed by crude extract ELISA, and 20 binders were sequenced. The results revealed five new EpCAM binders termed EPh2 to EPh6.

Expression, purification and specificity of the selected DARPins

The selected DARPins, including EPh1 with the small deletion, were expressed at high levels in soluble form in the cytoplasm of *E. coli* XL1-Blue (up to 140 mg/l in normal shake flasks). All proteins were purified by a single immobilized metal affinity

chromatography (IMAC) purification step. The specificity of the selected DARPins was determined by ELISA (Fig. 1). E3_5,¹ an unselected member of the DARPIn library without target specificity, served as a control and showed no binding to EpCAM or any of the control proteins.

EpCAM binding of selected DARPins on cells and EPh1 epitope characterization

We then investigated the ability of the selected binders to bind to EpCAM on the cell surface. To this end, the DARPins were genetically fused to superfolder green fluorescent protein (sfGFP)²² and analyzed for binding to EpCAM-positive MCF-7 cells using flow cytometry. DARPIn-sfGFP fusion proteins expressed very well and showed EpCAM-specific binding in ELISA (Supplementary Fig. 2a). It might be noted that, for antibody fragments, similar direct GFP fusion proteins can only be produced at much lower yields.²³ To assess whether GFP interfered with or unspecifically contributed to binding of the DARPins to EpCAM on the cell surface, we used two additional detection methods: (i) unfused DARPins were incubated with target cells and detected with a primary antibody (anti His-tag, located at the N-terminus) and a secondary fluorescein isothiocyanate (FITC)-labeled antibody using flow cytometry; (ii) EpCAM binders were cloned in a vector containing a C-terminal AviTag for *in vivo* biotinylation. The biotinylated binders were expressed, purified and incubated with streptavidin Alexa Fluor 488. The labeled DARPins were incubated with EpCAM-positive cells and detected using flow cytometry.

Flow cytometry indicated the same result for all three detection methods (Supplementary Fig. 2b). Whereas all selected DARPins showed specific binding to EpCAM in ELISA, only one, EPh1, was able to bind to EpCAM in its native conformation on the surface of MCF-7 cells. This was observed with all three approaches. DARPins that did not bind to native EpCAM on cells were not further evaluated. Their enrichment suggests

that epitopes are present on purified EpCAM, which are masked and thus inaccessible in the context of the plasma membrane.

To confirm that Eph1 binds to EpCAM on various tumor cell types, we investigated its binding to four additional EpCAM-positive cell lines of different histotypes (CAL27 squamous cell carcinoma of the tongue, SW2 small cell lung carcinoma, MCF-7 breast carcinoma, LNCAP prostate carcinoma and HT29 colorectal carcinoma) using flow cytometry. As shown in Fig. 2a, Eph1 bound to all EpCAM-positive cell lines, whereas no binding was detected on EpCAM-negative RL lymphoma cells.

The monoclonal antibody MOC31 binds to an epitope on the extracellular epidermal growth factor-like domain of EpCAM.²⁴ In competition binding experiments, Eph1-specific binding to EpCAM was reduced in the presence of MOC31 as measured by ELISA and flow cytometry (Fig. 2b and c). This indicates that their epitopes were at least partially overlapping. As a further control, it was shown that the soluble extracellular domain of EpCAM (EpEx) could compete the specific binding to immobilized bEpEx in ELISA.

Selection of EpCAM-specific DARPinS using ribosome display

To further increase our repertoire of EpCAM binders, we also used two different DARPIn libraries (N2C and N3C)¹ in ribosome display. Three selection rounds in solution were performed, and DARPins obtained after the third round of selection were analyzed for specific binding to bEpEx by crude extract ELISA. We identified seven EpCAM binders that belong to three distinct families defined by carrying the same or almost the same residues at randomized positions but different framework mutations. All sequences differed at the randomized positions from Eph1. The newly selected DARPins were fused to sfGFP and analyzed for binding to EpCAM by flow cytometry. All analyzed DARPins showed binding to EpCAM-positive but not EpCAM-negative cells (data not shown). While it is tempting to speculate that the greater size of the ribosome display library and the inherent diversification by random mutations in the ribosome display process contributed to the larger number of cell-binding clones, it is also possible that epitope masking employed in phage display significantly restricted the accessible space.

The mean fluorescence intensity (MFI), measured by fluorescence activated cell sorting (FACS), of the newly selected DARPins was lower when compared to the MFI of Eph1 (all tested at the same concentration) (data not shown). This difference might be due to lower affinities to EpCAM, either intrinsic or caused by differential accessibility of the recognized epitopes on the cell surface.

Optimization of binders using ribosome display

Eph1 and the previously ribosome display selected binders were subjected to directed evolution using error-prone polymerase chain reaction in the presence of dNTP analogs²⁵ followed by new rounds of off-rate selection using ribosome display in solution. The binders initially selected from ribosome display were in the mid-nanomolar range as estimated from competition ELISA.¹⁵ In contrast, Eph1 showed a much higher apparent affinity; however, it formed dimers and multimers (Fig. 3). This was not due to instability of the molecule but most likely to fortuitous self-complementarity of its surface (see data below). We were therefore interested whether this self-complementarity could also be eliminated by directed evolution.

To this end, we first replaced the C-cap of all EpCAM binders with a more stable recently designed version.⁵ After error-prone PCR, the pools were subjected to four or five rounds of selection by ribosome display using a combination of stringent and non-stringent rounds.²⁶ On the basis of crude extract ELISA signals and SDS-PAGE analysis, 92 clones were sequenced, resulting in 65 unique sequences. Sequence analysis revealed that 30 sequences (46%) were derived from Eph1: this group of binders maintained the same randomized positions and the characteristic two-amino-acid deletion as Eph1 but had different framework mutations. The rest of the evolved binders (33 sequences or 51%) were derived from different binders provided by the original ribosome display selection. Two binders could not be assigned to any family of input binders.

All 65 second-generation binders were expressed and purified in a 96-well format. Based on competition ELISAs, analytical size-exclusion chromatography and flow cytometry analysis, the seven best EpCAM binders were chosen (sequences shown in Supplementary Fig. 3). Five belonged to the Eph1 family and were named Ec1 to Ec5, and the other two binders were derived from binder C9 selected by the original ribosome display¹⁵ selection and were named Ac1 and Ac2.

Characterization of the evolved EpCAM binders

When binding to EpCAM was tested by competition ELISA, the signal was decreased for all seven binders when non-biotinylated EpCAM was used as competitor (Supplementary Fig. 4), as expected for specific binders. Moreover, when analyzed by gel filtration, Ac2 and Ec2 showed a small shoulder, which might correspond to a small amount of dimers (Fig. 3), but no aggregation was seen. The remaining five DARPins were entirely monomeric.

Interestingly, the ribosome display rounds initially employed for affinity maturation also removed the

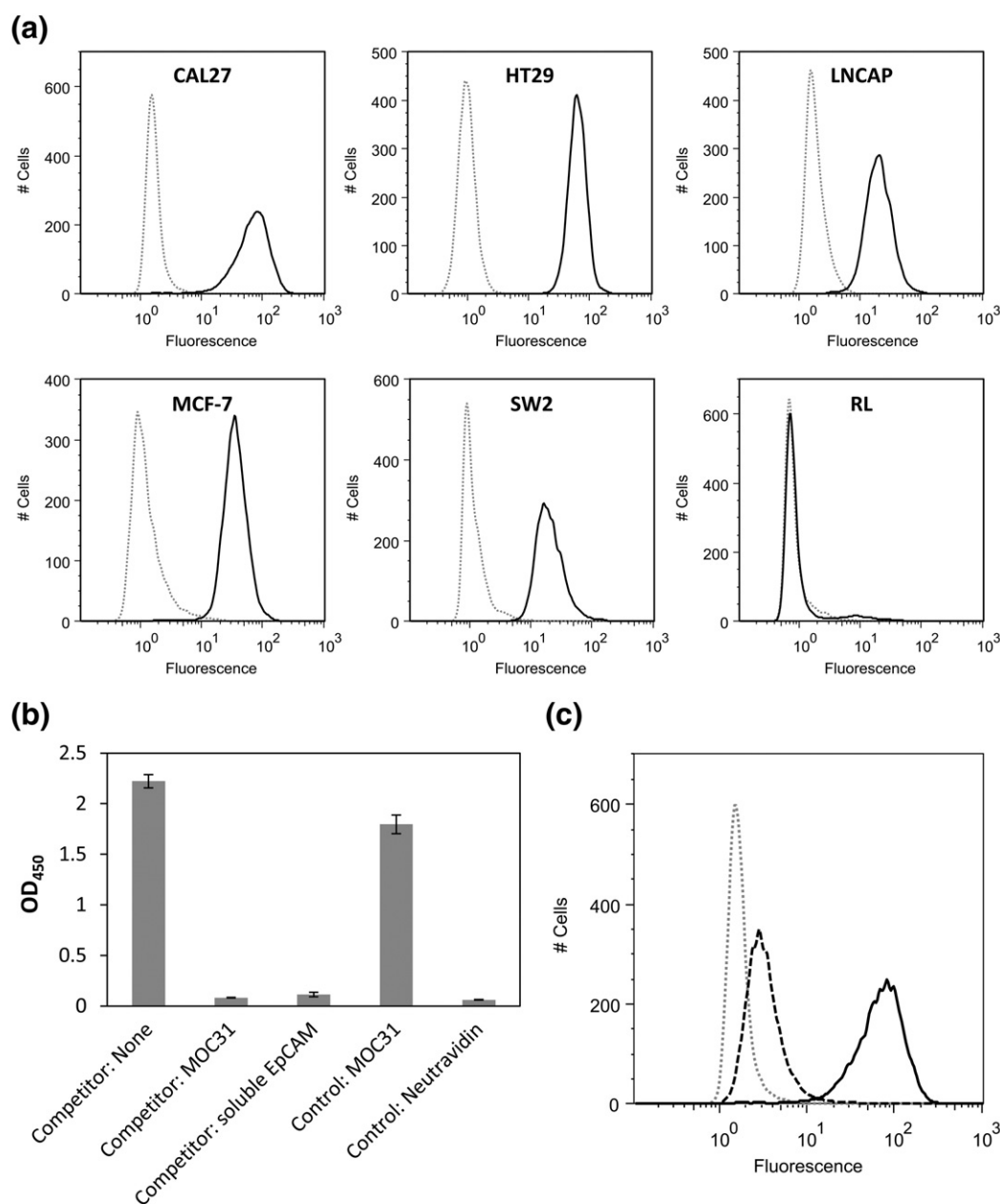


Fig. 2. (a) Binding of DARPin Eph1 to tumor cells analyzed by flow cytometry. Eph1 fused to sfGFP was incubated for 45 min at 4 °C with different EpCAM-positive tumor cell lines (CAL27, HT29, LNCAP, MCF-7 and SW2). The EpCAM-negative cell line RL was used as control. Fluorescence signals from Eph1-sfGFP are shown in black, and autofluorescence of cells is in a gray dotted line. (b) MOC31 competition—ELISA. Binding of Eph1 to immobilized EpCAM was competed with the monoclonal antibody MOC31 and with soluble non-biotinylated EpCAM. Biotinylated EpCAM (20 nM) was immobilized on neutravidin-coated plates, and binding of Eph1 (10 nM) was detected. Competition with a 10-fold excess of MOC31 (100 nM) or with soluble EpCAM (100 nM) was examined. MOC31 (100 nM) binding to bEpEx is included as positive control. Binding of Eph1 to neutravidin is shown as background control. (c) MOC31 competition—flow cytometry. Binding of Eph1 to CAL27 cells was competed with the monoclonal antibody MOC31. CAL27 cells (1×10^6 cells) were incubated with Eph1-sfGFP alone (black) or in the presence of an excess of MOC31 (broken). Autofluorescence from the cells is shown in a gray dotted line.

dimerization and oligomerization tendency of Eph1. To better understand the mechanism of this favorable selection outcome, we built homology models of Eph1 and selected mutants, based on the

structures of the full consensus DARPinS 2QYJ²⁷ (2.05 Å resolution) and 2XEE⁶ (2.10 Å resolution), using the homology module of InsightII (Accelrys Inc.). The two-amino-acid deletion in the hairpin

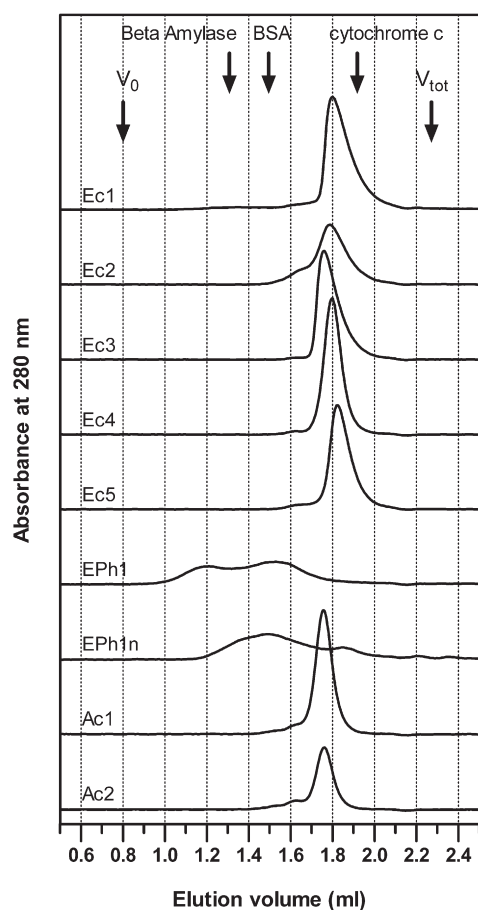


Fig. 3. Analytical gel filtration. DARPin (15 μ M, 50 μ l) was analyzed on an AKTA micro liquid chromatography system using a Superdex 200 column (both GE Healthcare). The molecular mass standards beta-amylase (200 kDa), BSA (66 kDa) and cytochrome *c* (12.4 kDa) as well as exclusion volume (V_0) and dead volume (V_{tot}) are indicated by arrows.

loop between the N-terminal capping repeat (N-cap) and the first internal repeat of EPh1 could be accommodated without undue strain. The model was analyzed using the Rosetta suite of programs.²⁸ Overall Rosetta scores (module fixbb, side-chain repacking with no mutations introduced) were marginally better for the models of the parental EPh1 than for the template structures, and none of the point mutations picked up during affinity maturation were predicted to have a significant stabilizing effect (Rosetta 3.1, module Rosetta 3.1, fix_bb_monomer_ddg). Twenty-two clones differing from the wild type by 0–9 mutations (average of 3.6 mutations) were modeled and analyzed. No correlation was found between the number of mutations, their predicted effects on thermodynamic stability and the observed aggregation behavior of the mutants, despite the fact that some of the individual point

mutations were predicted to have a significant *destabilizing* effect.

For testing of the predictions made by Rosetta calculations experimentally, circular dichroism (CD) spectra were recorded (Supplementary Fig. 5), and thermal denaturation was monitored at 222 nm (Supplementary Fig. 6). The original EPh1 with some aggregation tendency shows a helical CD spectrum with somewhat smaller intensity and a flatter line in the thermal denaturation, but no thermal transition. EPh1n, whose aggregation tendency is already reduced by the reengineered C-cap but is still not monomeric (Fig. 3), shows the same helical spectrum as the evolved mutants (Supplementary Fig. 5). Interestingly, several of the evolved mutants, but not the starting clone EPh1n, now show an unfolding transition in the range of 80–95 °C (Supplementary Fig. 6). Also, expression levels of EPh1 and its mutants in *E. coli* were within the range expected for DARPins (150–200 mg/l shake flask culture). Collectively, these data argue against the hypothesis that the EPh1 deletion has destabilized the DARPin, which would have led to the aggregation of misfolded molecules, and that the optimization process using ribosome display would have selected for compensating mutations that stabilize the native structure.

A more plausible, alternative explanation for EPh1 aggregation would be a non-negligible binding affinity of *native* EPh1 molecules for each other. Indeed, the results of ELISA experiments testing the binding of EPh1 to EPh1 and other DARPins (Supplementary Fig. 7) are consistent with dimerization and multimerization of EPh1 being a consequence of fortuitous self-complementarity of the surface of this fully native stable DARPin molecule. Ribosome display might thus have selected for molecules without self-complementarity, as they increase the percentage of molecules available for target binding. This selection even caused some destabilization, but unfolding transitions around 90 °C are not an impediment for any application. The fact that ribosome display can “remove” self-complementarity and enrich monomers was unanticipated but may be very useful.

The ability of the seven DARPins to interact with EpCAM on the cell surface was determined by flow cytometry. All DARPins bound to EpCAM-positive cells (Fig. 4a) but not to EpCAM-negative control cells (Fig. 4b). The unselected DARPin E3_5 did not interact with any of the cell lines tested.

We next examined whether the two families bind to different EpCAM epitopes by flow cytometry. To this end, binding of Ec4-sfGFP in the presence of an excess of Ac2 and binding of Ac2-sfGFP in the presence of an excess of Ec4 to MCF-7 cells were analyzed (Fig. 4c). Since no mutual competition was observed, we conclude that the two families recognize nonoverlapping epitopes. In addition,

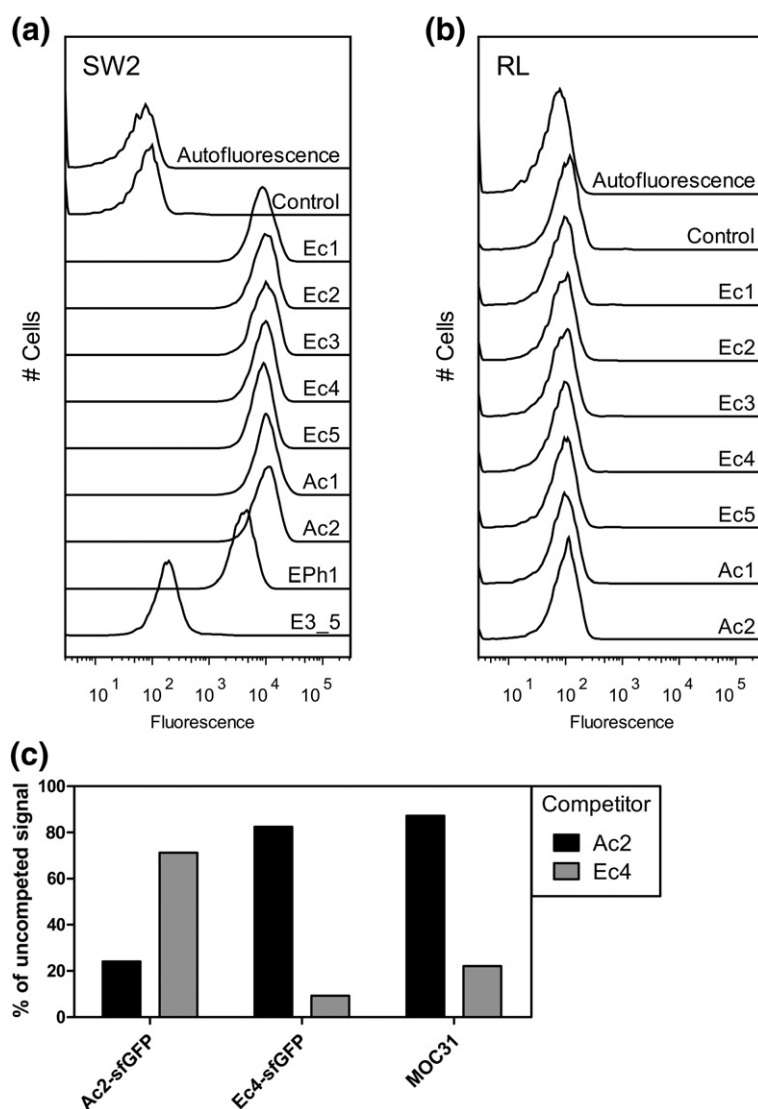


Fig. 4. Analytical flow cytometry. (a) EpCAM-positive SW2 cells or (b) EpCAM-negative RL cells were incubated at 4 °C with the EpCAM-specific DARPins for 1 h. Binding was detected with a mouse anti-RGS(His)₄ as primary and Alexa Fluor 488-coupled goat anti-mouse IgG as secondary antibody. Control: primary and secondary antibodies only; E3_5: unselected DARPin library member (negative control). (c) Flow cytometric competition assay. 5×10^5 HT29 cells were incubated with 10 μ M unlabeled DARPin Ac2 or Ec4 for 15 min on ice before 100 nM Ec4-sfGFP or Ac2-sfGFP fusion proteins or the monoclonal antibody MOC31 were added for 30 min. MOC31-treated samples were additionally incubated with 2 μ g/ml (13.3 nM) Alexa Fluor 488 goat anti-mouse IgG for 20 min on ice. Samples were then analyzed by flow cytometry. MFI values in the FITC channel were normalized to cells not preincubated with competitor.

Ec4 (like its predecessor Eph1) competed for binding with the anti-EpCAM antibody MOC31, whereas Ac2 did not.

Affinity determination

We determined the equilibrium dissociation constant (K_d) of all seven molecules that were further characterized (Ec1–5 and Ac1 and Ac2), by surface plasmon resonance (SPR) with purified bEpEx (Supplementary Fig. 8). The highest affinity was measured with Ec1, a pure monomer for which an association rate of $3.57 \times 10^5 \text{ M}^{-1} \text{ s}^{-1}$ and a dissociation rate of $2.44 \times 10^{-4} \text{ s}^{-1}$ resulted in a K_d of 68 pM (Table 1). We measured an affinity of 86 pM for Eph1, but we cannot ascertain whether binding is truly monovalent in this partially self-complementary molecule, when taking the gel-filtration profile of this protein into consideration.

To determine the affinity for EpCAM on cells, we performed flow cytometry of Alexa Fluor 488-labeled Ec1 and Ec4 with MCF-7 cells using the determination of association and dissociation rates on cells^{12,29} under conditions where internalization was minimized. The calculated affinity on cells was 0.37 nM and 10.3 nM, respectively (Fig. 5). The difference in affinities to SPR measurements was entirely due to a slower k_{on} , whereas the dissociation rate constant k_{off} was almost identical in both experimental setups (Table 1). It is likely that this lower on-rate was due to a limited accessibility of the cognate epitope on the cell surface.

Ac1 and Ac2 displayed affinities in the low nanomolar range (Fig. 6, Supplementary Fig. 9 and Table 2). Interestingly, the dissociation phase appeared to be biphasic, consisting of a fast phase and a slow phase both in SPR and on cells. To measure unspecific binding, we also performed equilibrium and dissociation experiments after

Table 1. Association and dissociation kinetics and affinities of selected DARPinS

Binder	SPR			Flow cytometry				
	Kinetic			Kinetic			Equilibrium	
	k_{on} ($\text{M}^{-1} \text{s}^{-1}$)	k_{off} (s^{-1})	K_{d} (M)	k_{on} ($\text{M}^{-1} \text{s}^{-1}$)	k_{off} (s^{-1})	K_{d} (M)	Saturation K_{d} (M)	Competition K_{d} (M)
Ec1	3.6×10^5	2.4×10^{-5}	6.8×10^{-11}	5.7×10^4	2.1×10^{-5}	3.7×10^{-10}		
Ec2	3.2×10^5	3.5×10^{-4}	1.1×10^{-9}					
Ec3	2.1×10^5	2.6×10^{-4}	1.3×10^{-9}					
Ec4	1.5×10^5	3.1×10^{-4}	2.1×10^{-9}	4.1×10^4	4.2×10^{-4}	1.1×10^{-8}	3.8×10^{-9}	7.5×10^{-9}
Ec5	2.8×10^5	5.0×10^{-5}	1.8×10^{-10}					
EPh1	3.5×10^5	3.0×10^{-5}	8.6×10^{-11}					
EPh1n	4.0×10^5	2.3×10^{-5}	5.7×10^{-11}					
Ec4-LZ					1.9×10^{-4}			
Ec4-LZ-off7					1.8×10^{-4}			
Ec4-LZ-Ec4					2.0×10^{-5}			
Ac2-LZ-Ec4					2.0×10^{-5}			
Ec4-LZ-Ac2					7.8×10^{-6}			
Ec1-LZ-Ac2 ^a					$<1.0 \times 10^{-6}$			

^a no dissociation detected.

blocking Ac-family epitopes with an unlabeled tetravalent Ec1-LZ-Ac2 (see below). Subtraction of the unspecific signal confirmed the presence of fast and slowly dissociating parts, the latter accounting for approximately 20% of Ac2-EpCAM complexes.

Multivalent constructs

To generate high-affinity binders that dissociate from EpCAM even more slowly, we constructed bivalent and tetravalent fusion proteins. Since DARPinS can be linked at both the N- and C-termini, head to tail (via a flexible linker), head to head (via an N-terminal dimerization module) or tail to tail (via a C-terminal dimerization module), multivalency can be readily adapted to the receptor arrangement on target cells. Through fusion of DARPinS to either end of a dimerization module, all three possibilities are combined in a single molecule, allowing even greater variation when combining more than one DARPin. In a first proof-of-principle experiment using a first-generation DARPin, we could indeed demonstrate that homo-dimerization already has potential to improve drug delivery.¹⁵ Here, we wanted to extend this further by making use of different epitope binders.

Multivalency was achieved by linking one or two DARPinS via a leucine zipper domain derived from GCN4 (Fig. 7a). Dissociation of these multivalent proteins from cells was followed indirectly by measuring the association of labeled monovalent DARPin to MCF-7 cells previously saturated with unlabeled multivalent binder (Fig. 7b and c). Whenever a site on EpCAM becomes accessible through (slow) dissociation, it is immediately occupied by labeled monomeric DARPin present at high concentration and whose association rate is thus not rate-limiting.

The dissociation rate of monovalent DARPinS we obtained in direct and indirect experimental setups was identical, demonstrating that the indirect method is robust. Through the use of Ec4-sfGFP as competitor, a k_{off} of $3.69 \times 10^{-4} \text{ s}^{-1}$ was determined for monomeric Ec4, and the dissociation rate was reduced 2-fold for Ec4-LZ (bivalent) and 18-fold for Ec4-LZ-Ec4 (tetravalent) (Table 1). The greatest reduction of 47-fold was observed for Ec4-LZ-Ac2, whereas Ac2-LZ-Ec4, the tetravalent construct with the positions of the two binders swapped, had an only 18-fold slower k_{off} (Fig. 7b). These extremely low off-rates were only observed when binders from both sequence families (i.e., binding to different epitopes) were combined into the same molecule. This is most clearly seen when using Ac2-sfGFP as competitor: Only Ec4-LZ-Ac2 could prevent the association of Ac2-sfGFP, while Ac2-LZ-Ec4 could not (Supplementary Fig. 10). Therefore, these new multispecific molecules greatly extend the previously reported bivalent binders, which only target a single epitope (see Discussion).¹⁵

For multivalent proteins containing the picomolar binder Ec1 (binding to the same epitope as Ec4), whose off-rate from cells is already so slow that it is hardly measurable, further improvement with the analogous tetravalent Ec1-LZ-Ac2 could not be directly assessed (Fig. 7c). However, the improvement can be expected to be in a similar range as for Ec4 and Ec4-LZ-Ac2, and the k_{off} should thus be clearly below 10^{-6} s^{-1} .

Detection of internalization by confocal microscopy

Since DARPinS might be useful for intracellular delivery of anticancer agents, we explored if EPh1, the first-generation molecule, is efficiently internalized

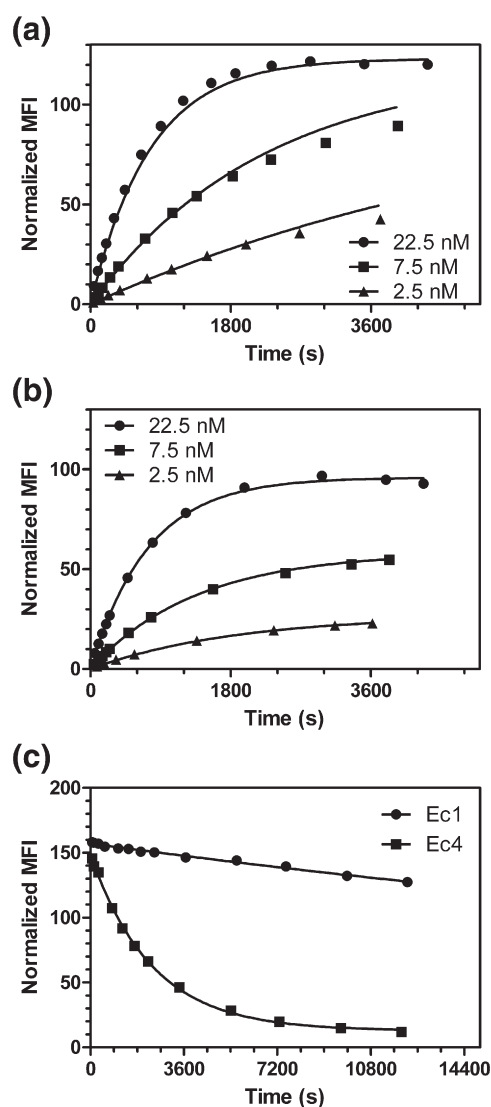


Fig. 5. Association and dissociation of fluorescently labeled DARPins from EpCAM-positive MCF-7 cells. (a) Association of Ec1, (b) association of Ec4 and (c) dissociation of Ec1 and Ec4. DARPins were labeled with Alexa Fluor 488 at a C-terminal cysteine. For dissociation measurements, cells were incubated with 100 nM fluorescently labeled Ec1 or Ec4 for 1 h at 4 °C, washed and resuspended in 1 μ M unlabeled Ec1 or Ec4 ($t=0$) to prevent rebinding. For association measurements, cells were resuspended in 2.5, 7.5 and 22.5 nM fluorescently labeled Ec1 or Ec4 ($t=0$). MFIs measured on a FACScanto II analytical flow cytometer (BD Biosciences) at different time points with unlabeled cells were set to 1 and used to calculate k_{on} , k_{off} and K_d . Results are summarized in Table 1.

upon binding to EpCAM on the cell surface. To this end, Eph1 was labeled with Alexa Fluor 488 and added to MCF-7 cells at 37 °C (to enable receptor internalization) or at 4 °C (to prevent internalization). Cells were examined using a confocal microscope to monitor subcellular localization of the DARPin

(Supplementary Fig. 11). The staining pattern obtained at 4 °C showed predominantly diffuse surface membrane fluorescence, whereas at 37 °C, bright punctuated dots are seen, which likely represent internalized DARPins in endo-/lysosomes.

Similarly, two of the evolved molecules, one of each sequence family, were tested, resulting in a similar staining pattern as observed with the parental DARPins (Fig. 8). No staining was visible when cells were preincubated with unlabeled binders or when the unrelated DARPin Off7 fused to Alexa Fluor 488 was used. This shows that efficient internalization was specific, that it is obtained with the monomeric DARPins and presumably reflects spontaneous internalization of EpCAM.

***In vitro* cytotoxicity of DARPin-based fusion toxins**

To test whether the ability of EpCAM DARPins to rapidly internalize in cells can be employed for

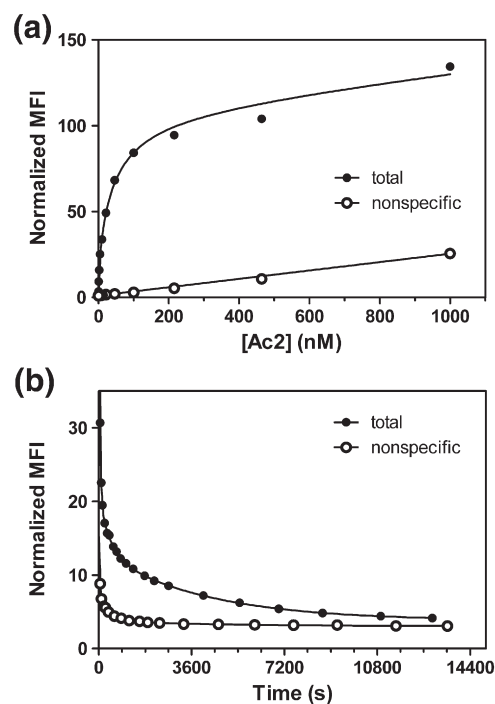


Fig. 6. Equilibrium binding and dissociation of fluorescently labeled Ac2 from EpCAM-positive MCF-7 cells. (a) Cells were incubated for 45 min at 4 °C with different concentrations of Ac2 coupled to Alexa Fluor 488 at a C-terminal cysteine. (b) For dissociation measurements, cells were incubated with 1 μ M fluorescently labeled Ac2 for 45 min at 4 °C, washed and resuspended in 5 μ M unlabeled Ac2 ($t=0$) to prevent rebinding. In both experiments, values for nonspecific binding were obtained by preincubating the cells for 60 min at 4 °C with 5 μ M tetravalent Ec1-LZ-Ac2. MFIs were measured on a FACScanto II analytical flow cytometer (BD Biosciences). Results are summarized in Table 2.

Table 2. Association and dissociation kinetics and affinities of Ac-series DARPins

Binder	SPR						
	Kinetic						Equilibrium
	k_{on1} ($M^{-1} s^{-1}$)	k_{off1} (s^{-1})	K_{d1} (M)	k_{on2} ($M^{-1} s^{-1}$)	k_{off2} (s^{-1})	K_{d2} (M)	K_d (M)
Ac1	1.0×10^6	1.2×10^{-4}	1.2×10^{-10}	1.1×10^6	8.0×10^{-2}	7.5×10^{-8}	4.8×10^{-8}
Ac2	5.6×10^4	8.0×10^{-5}	1.4×10^{-9}	6.9×10^5	9.0×10^{-2}	1.3×10^{-7}	1.3×10^{-7}
Binder	Flow cytometry						
	Kinetic						Equilibrium
	k_{on1} ($M^{-1} s^{-1}$)	k_{off1} (s^{-1})	K_{d1} (M)	k_{on2} ($M^{-1} s^{-1}$)	k_{off2} (s^{-1})	K_{d2} (M)	K_d (M)
Ac2	1.6×10^4	2.5×10^{-4}	1.6×10^{-8}	4.8×10^5	2.6×10^{-2}	5.5×10^{-8}	2.2×10^{-9}

intracellular delivery of anticancer agents, we fused them via a (GSG₄)₂S linker to a truncated form of *Pseudomonas* exotoxin A (ETA"). We recently presented the cytotoxic potency and antitumor effect of a fusion toxin for one of the selected DARPins, Ec4, in mice.¹⁶ Here, we generated ETA" fusion toxins with all the selected EpCAM binders and compared their cytotoxic potency and that of the control E3_5-ETA" on EpCAM-positive HT29 cells in XTT cell viability assays. We wanted to specifically investigate a relationship between affinity and activity. Cytotoxicity was determined in colorimetric XTT cell viability assays upon 72 h of exposure. As expected, all EpCAM binding fusion toxins showed an IC₅₀ value (concentration at which cell viability was reduced by 50%) orders of magnitude lower than that of the unspecific E3_5-ETA", indicating EpCAM-specific receptor-mediated endocytosis. Specificity through evolution was maintained, since cytotoxicity was substantially decreased when cells were preincubated with an excess of the corresponding unfused DARPin as competitor. The lowest IC₅₀ values were obtained for Ec5-ETA" (39 fM), which is almost 100,000-fold lower than that of the unspecific E3_5-ETA" (Fig. 9) and about 4.4-fold better than that of Ec4, which had been used previously, after only preliminary *in vitro* characterization.¹⁶ In the cell culture experiments reported here, for toxins fused to DARPins with higher affinity (e.g., Ec1 and Ec5), indeed lower IC₅₀ values were observed than for those fused to binders of lower affinity.

In summary, the evolution of the DARPins, where a case of spurious self-recognition could be removed through ribosome display selection, led to binders with high affinity and selectivity. Their combination to a format with four DARPins, which is bispecific and tetravalent in each binding site, led to molecules with an immeasurably small off-rate on cells.

Discussion

We show in this study the generation, evolution and characterization *in vitro* and on cells of specific

binders from a DARPin library against the tumor-associated antigen EpCAM. EpCAM is widely expressed on solid tumors, particularly also on tumor-initiating cells, and efficiently internalized by receptor-mediated endocytosis. It thus perfectly matches the need of tumor targeting with anticancer agents acting on intracellular targets such as DNA damaging agents, toxins, antisense oligonucleotides and small interfering RNA (siRNA).^{15,30–32}

Phage display and ribosome display

Using the purified extracellular domain of EpCAM expressed in HEK293T cells, we employed two different selection techniques: SRP phage display and ribosome display. Both selection techniques were found to be well suited for the *in vitro* selection of binders from synthetic DARPin libraries yet resulted in different sequence families. This is, in part, probably due to the fact that no library selection is ever exhaustive. Both DARPin libraries used here ultimately come from the same material: The phage display library was PCR amplified from the ribosome display library in the N3C format.¹¹ Thus, it can be considered an "aliquot" of 2.6×10^{10} clones of the total DARPin diversity constructed, while each ribosome display panning experiment uses an aliquot of about 10^{11} to 10^{12} molecules from the pool. It is thus, per se, not surprising to find different clones in the two approaches, and it would be very difficult to pinpoint this to the different "aliquots" used, the selection system per se or differences in the immobilization used. What is clear, however, is that varying these parameters does increase the diversity of hits.

Ribosome display removes self-complementarity in a binder

From the initial selection by phage display on immobilized EpCAM, we found one dominant binder, named EPh1, presenting a characteristic two-amino-acid deletion between the N-terminal capping repeat and the first internal repeat (Supplementary Fig. 3). This deletion was not observed in

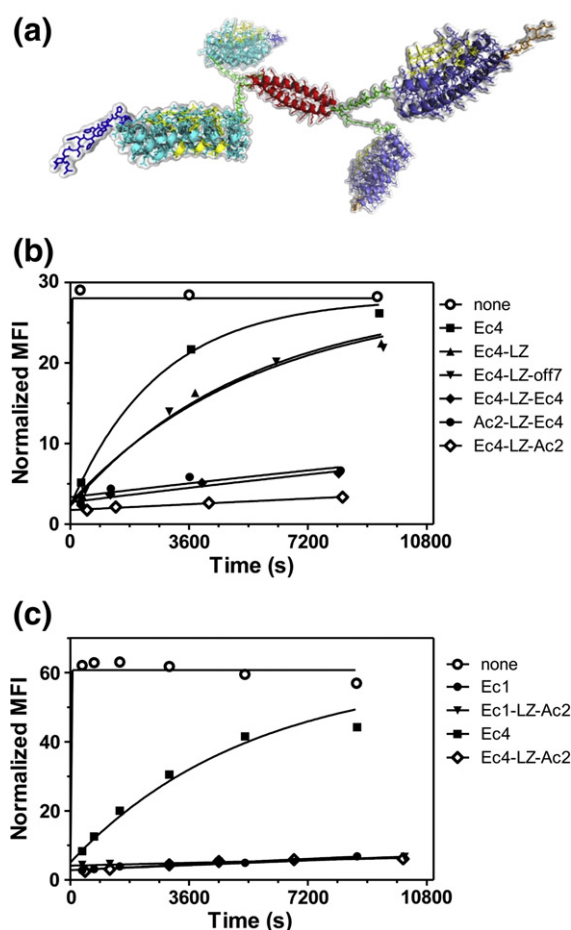


Fig. 7. Multivalent DARPinS. (a) Model of DARPinS (cyan and purple, randomized positions in yellow) that were N- and C-terminally fused to a leucine zipper dimerization domain (red) derived from GCN4 via short flexible peptide linkers (green). The N-terminal MRGSH₆ tag is indicated in dark blue, and the C-terminal sequence (RSDLDTGLKLN) is in orange. For indirect measurement of dissociation rates from MCF-7 cells, 6×10^5 cells in 1 ml were saturated for 1 h at 4 °C with 200 nM unlabeled DARPin. Then, cells were centrifuged and resuspended with 2 μ M Ec4-sfGFP (b) or Ec1-sfGFP (c). Association of the labeled monovalent binder was measured at different time points between 0 and 4 h and occurred at the rate of dissociation of unlabeled DARPin. Results are summarized in Table 1.

other selections performed with the same library. The deletion, which most likely happened in one or a few molecules already in the original assembly of the library from synthetic oligonucleotides and was found in the phage display aliquot, is a very rare event, leading in this case to a valuable clone. It appears to favor binding to a particular epitope, since when the two amino acids were reinserted, binding affinity was significantly reduced. Selection of only one dominant binder or a low diversity of binders selected on certain target proteins is a common

phenomenon observed with phage display.¹¹ This particular clone appeared to show fortuitous self-complementarity, unrelated to its two-amino-acid deletion, as it could be completely removed during further maturation by ribosome display, thus demonstrating an unexpected feature of this selection technology.

The ribosome display maturation thus maintained not only the same randomized positions but also the characteristic two-amino-acid deletion found in Eph1 and resulted in four to six different framework mutations. These framework mutations eliminated any self-association tendency that the precursor Eph1 had. In contrast, none of the DARPins with

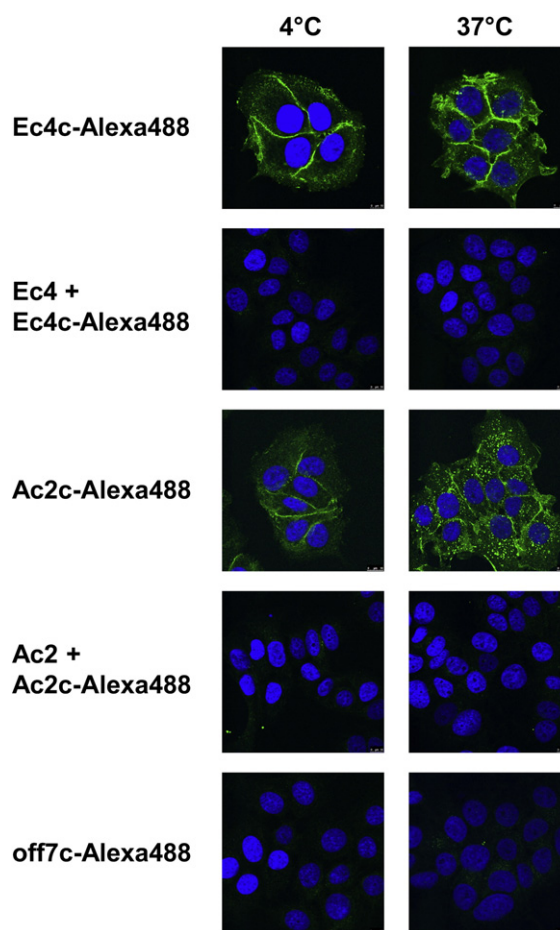


Fig. 8. Internalization of EpCAM binders visualized by confocal microscopy. For competition binding, MCF-7 cells were preincubated with unlabeled EpCAM binders, Ec4 and Ac2. Then, EpCAM-specific DARPins, Ec4 and Ac2, and the unspecific DARPin off7, all labeled with Alexa Fluor 488, were added to the cells. After 1 h of incubation at 37 °C or at 4 °C, cells were washed and fixed with 4% paraformaldehyde, and nuclei were stained with 4',6-diamidino-2-phenylindole. Fluorescent images were recorded using a confocal laser scanning microscope (TCS-SP 2; Leica Mannheim) with a selected confocal plane positioned approximately in the middle of the cell.

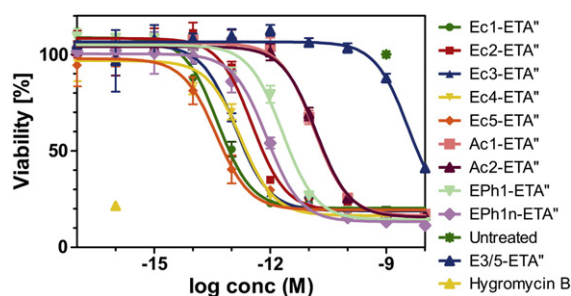


Fig. 9. Cytotoxicity of the DARPin-based fusion toxins. The cytotoxicity of the various EpCAM-specific ETA fusion toxins and the irrelevant control fusion toxin E3_5-ETA was tested on EpCAM-positive HT29 colon carcinoma cells using a colorimetric XTT cell viability assay. Cells were incubated in the presence of the fusion toxins for 72 h before viability was determined.

self-association tendency bears substitutions in these positions. We did not identify a mutation common to all monomeric DARPins, indicating that self-binding can be prevented in different ways. It is this self-complementarity that makes Eph1 itself not a very useful molecule for biomedical applications.

The evolved proteins (Ec series) were pure monomers. Analysis by Rosetta and in experimental melting curves gave no indication that Eph1 had any amino acids problematic for folding or stability that were “corrected” but, on the contrary, that some of the evolved molecules were slightly *destabilized* (from showing no transition in the measured range to a melting transition around 90 °C). Thus, we postulate that, in Eph1, *native* molecules show self-complementarity, and directed evolution could eliminate these surface features while still improving binding. Thus, residues responsible for self-complementarity could apparently be separated from those involved in binding the target. The ultimate explanation will have to await the solution of the crystal structure of the complexes.

ELISA data support the self-binding hypothesis (Supplementary Fig. 7), as the strongest signals were detected for mixtures of biotin-Eph1 and Eph1n-hemagglutinin (HA), the HA-tagged parental binder with the stability-improved C-terminal capping repeat. Interestingly, signals of biotin-Eph1 interacting with Eph1-HA (with the original C-cap) were at background level, which might be explained by a lower active concentration of Eph1-HA due to self-association.

Targeting new epitopes

To increase the repertoire of binders, we employed epitope masking to recover binders recognizing other epitopes.²¹ The five new binders so obtained specifically recognized EpCAM in ELISA but failed to bind to EpCAM expressed on

the cell surface, and only Eph1 was capable of binding to EpCAM expressed on different tumor cells. It is possible that isolated EpCAM may have exposed additional epitopes not accessible on the cell, as EpCAM is oligomerizing and associating with other molecules in the plasma membrane.²⁴ For example, EpCAM can interact with the tight junction protein claudin-7 followed by recruitment into tetraspanin-enriched membrane microdomains where it is complexed with tetraspanin and CD44v6.³³ Additionally, blocking the preferred epitope on EpCAM may render even closely adjacent binding sites inaccessible.

Ribosome display selection using an N2C and an N3C DARPin library 1 resulted in seven new binders that belong to three families. None of these families featured the same randomized positions as Eph1 or its two-amino-acid deletion. All binders selected by ribosome display were capable of binding to EpCAM in its native conformation on cells. One of these first-generation DARPins, C9, which showed intermediate affinity, was already tested to explore its potential for tumor targeting in form of a fusion protein with protamine, complexed with proapoptotic siRNA.¹⁵ Here, we used error-prone PCR with stringent selection by ribosome display on all binders (the one from phage display above plus the initially found ones from ribosome display) to improve their affinities.⁹ Of the finally chosen seven binders, two were derived from the ribosome display pool (Ac series; the Ec series derived from phage display is described above). Similar to their parental binder C9, these DARPins bind to EpCAM with affinity in the nanomolar range. However, their association and dissociation appeared to be biphasic, consisting of a large fraction with fast kinetics and a small fraction with slow dissociation kinetics. This slowly dissociating portion could explain why these binders were not lost during off-rate selection and why the molecules were selected like ones with low nanomolar affinity. We speculate that the epitope recognized by this sequence family is present on EpCAM in two different conformations that are recognized with different affinities.

Utility of the evolved EpCAM binders

Three of the evolved binders, Ec1, Ec4 and Ac2, were characterized on cells in detail. We had recently developed a method to determine even high functional affinities on cells by using on- and off-rates.^{12,29} Here, we extend this method by using a competition approach. This kinetic approach allows a direct comparison with SPR measurements. The binding of the evolved DARPins on cells showed a slower on-rate than measured by SPR, leading to a subnanomolar K_d on cells, while it is even mid-picomolar in SPR measurements (Fig. 5 and Table 1).

Ec4, Ec1 and Ac2, similarly to their parental binders, Eph1 and C9, are efficiently internalized into cells upon EpCAM binding, which is mandatory for delivering anticancer agents acting on intracellular targets.^{15,16} While we recently already reported that one of the DARPinS as a fusion toxin demonstrated efficient tumor localization and potent antitumor activity upon systemic administration,¹⁶ we now showed that we have DARPinS with higher activity on cells than employed in that study.

An important possibility to further improve performance on multi-domain receptors on cells is to exploit multivalency. This can target neighboring receptor molecules, subunits from a dimeric receptor or different epitopes in the same receptor molecule. Since with DARPinS, engineering and expression of such molecules are straightforward, we investigated these options with the new anti-EpCAM DARPinS.

We previously only had a medium-affinity first-generation DARPin available, C9, which we had fused to protamine and dimerized to increase its avidity for delivery of nanocomplexed siRNA into cells. This molecule, C9, is a precursor of the Ac family. Since selections yielded DARPinS also of the Ec family, recognizing a different epitope on EpCAM, we were now able to further enhance the functional affinity of the binders on cells by generating bivalent and tetravalent constructs based on fusion to a self-associating leucine zipper domain. Flow cytometry experiments showed that this multimerization in the case of Ec4-LZ-Ac2 enhanced the binding activity due to an up to 47-fold decrease in the dissociation rate. For a similar construct with the picomolar binder Ec1 whose off-rate was already too slow to measure, we could not directly measure the further decrease in rate by multimerization, but if the same avidity increase would hold, Ec1-LZ-Ac2 would bind to EpCAM on cells with functional affinity in the femtomolar range.

Importantly, these results also indicate that the epitope recognized by the Ac family was also efficiently blocked by the Ec-LZ-Ac configuration. Constructs equivalent to the previously reported C9 dimers,¹⁵ and even other bivalent and tetravalent constructs with Ac2 at the N-terminus only slightly decreased the dissociation rate over Ac2 itself (Supplementary Fig. 10). This shows the enormous avidity gain that is possible by combining binders to different epitopes and the important role of correct geometric arrangement. Since normally crystal structures of complexes will not be available early in such a project, it is advantageous that with the DARPinS, different constructs can be built and tested rapidly, since they all express reliably at about the same high level as monomers.

Therefore, such rationally engineered multimeric high-affinity DARPin constructs may provide a new

generation of ligands useful to, for example, interfere with receptor arrangement in the cell membrane and thus cell growth signaling or deliver conjugated anticancer payloads with high efficiency.

Conclusions

In summary, we could demonstrate the benefit of using both phage display and ribosome display to select binders against the clinically approved tumor antigen EpCAM, a highly glycosylated protein on tumor cells, with only few accessible epitopes. By combining both selection methods and subsequent stringent directed evolution, we generated high-affinity DARPinS to nonoverlapping epitopes of EpCAM. Ribosome display was capable of removing self-complementarity in the proteins and thus led to high-affinity binders with monomeric behavior, which expressed in high yield and could be easily purified. Moreover, since these binding proteins can be linked to each other in many geometries, they can be optimally adapted to the spatial arrangement required for optimal binding to the target epitope and can still be expressed and purified just as efficiently. DARPinS may thus provide the basis for a new generation of protein therapeutics for tumor targeting that are superior to antibodies in terms of stability, production, biophysical properties and freedom for engineering and optimization.

Materials and Methods

Cell lines and culture conditions

The colorectal carcinoma cell line HT29, the breast carcinoma cell line MCF-7, the non-Hodgkin's lymphoma cell line RL, the squamous cell carcinoma cell line of the tongue CAL27, the prostate carcinoma cell line LNCAP and the human embryonic kidney cells HEK293T were obtained from American Type Culture Collection (Manassas, USA). The small cell lung carcinoma cell line SW2 was maintained in our laboratory. All cell lines were grown in Dulbecco's modified Eagle's medium (DMEM) (Sigma, Buchs, Switzerland). Culture medium was supplemented with 10% heat-inactivated fetal bovine serum (Amimed, Bioconcept, Allschwil, Switzerland), 100 IU/ml penicillin and 100 µg/ml streptomycin (Sigma). Cell cultures were maintained at 37 °C in a humidified atmosphere containing 5% CO₂. All cells were tested negative for mycoplasma using MycoAlert (Lonza, Basel, Switzerland).

EpCAM expression and purification

The extracellular domain of EpCAM (EpEx), residues 1–265 (including the signal sequence), was cloned into the plasmid pCDNA3.1(–) for mammalian cell

expression. Two additional tags were added to the C-terminus of the protein, an Avi-tag (GLNDIFEAQ-KIEWHE) for biotinylation, followed by a His₆ tag for protein detection and purification. The expression vector was transfected into HEK293T cells using the standard calcium precipitation protocol. Four days after transfection, cell culture media were collected, centrifuged and filtrated to eliminate cell debris.

The supernatant containing EpEx was concentrated and loaded on an IMAC column packed with Ni-NTA super-flow (Qiagen, Hilden, Germany). After washing with 5 column volumes [50 mM NaH₂PO₄ (pH 8.0), 500 mM NaCl, 10% glycerol and 10 mM imidazole], EpEx was eluted with 50 mM NaH₂PO₄ (pH 8.0), 300 mM NaCl, 10% glycerol and 250 mM imidazole. After purification, EpEx was dialyzed against 10 mM Tris and enzymatically biotinylated. One milligram of protein (at a concentration of 1 mg/ml) was incubated with 10 µg of BirA (Avidity, Aurora, CO, USA) at room temperature overnight in a buffer containing 50 mM bicine (pH 8.3), 10 mM ATP, 10 mM Mg(CH₃COO⁻)₂ and 40 µM biotin. Biotinylated EpEx (bEpEx) was dialyzed against phosphate-buffered saline (PBS) [15 mM KH₂PO₄ (pH 7.4), 81 mM Na₂HPO₄, 27 mM KCl and 137 mM NaCl] to remove unreacted biotin. Efficient biotinylation was confirmed by using ELISA and Western blotting and detection with a streptavidin-horseradish peroxidase conjugate as detection reagent (Roche, Basel, Switzerland).

Selection of DARPins by SRP phage display and epitope masking

The selection of EpCAM-specific DARPins by phage display was performed essentially as previously described.¹¹ For the first selection round on immobilized target protein, 66 nM neutravidin (Pierce, Rockford, USA) was coated on MaxiSorp immunotubes (Nunc, Roskilde, Denmark). Tubes were blocked with PBSTB [PBS, 0.1% Tween-20 and 0.2% bovine serum albumin (BSA)] for 1 h, and bEpEx (1 ml, 400 nM) was added for 2 h at 4 °C. The second and third rounds were performed on MaxiSorp plates (Nunc). The plates were coated with neutravidin (Pierce) or streptavidin (Sigma) (66 nM, 100 µl/well in PBS) at 4 °C overnight. After washing, bEpEx (100 nM, 100 µl/well) was added for 1 h at 4 °C. To avoid selection of binders against neutravidin or streptavidin, we used these two proteins alternately in subsequent rounds. At the end of the third round, enrichment of specific binders was monitored by phage ELISA.

For epitope masking, DARPin Eph1 was expressed in *E. coli* and purified by IMAC as described below (purification of DARPins). Pools of phage particles after the first round on immobilized protein (in tubes) were used as input material. bEpEx (100 nM) was incubated with DARPin Eph1 (10 µM) for 1 h before a standard selection round on soluble protein was performed by which complexes of phages bound to bEpEx were captured with streptavidin-coated paramagnetic beads (Dynabeads MyOne Streptavidin T1, DYNAL; Invitrogen, San Diego, USA) for 20 min. After three rounds of selection with epitope masking, phage enrichment was analyzed by phage ELISA in the presence or absence of an excess of Eph1.

Phage ELISA

Phage ELISA was performed to detect specific enrichment of phages against EpCAM. Neutravidin (66 nM), streptavidin (66 nM) and human IgG1 Fc domain (negative control) (100 nM) were directly coated to MaxiSorp plates (Nunc) overnight at 4 °C. Biotinylated proteins, bEpEx (100 nM) and ErbB4 (negative control) (100 nM), were coated via neutravidin for 1 h at 4 °C. Output phages from each round ($\sim 1 \times 10^5$ phages) were incubated with the target and control proteins for 2 h at room temperature. After three washes with PBST (PBS and 0.1% Tween-20), bound phages were detected with mouse anti-M13 antibody horseradish peroxidase conjugate (Glattbrugg/Zürich, Switzerland).

Selection of DARPins by ribosome display

Both N2C and N3C DARPin libraries¹ were used to select for DARPins binding to EpEx. Three rounds of selection by ribosome display were performed essentially as described before.⁸ Briefly, for each round, the translation mix containing mRNA-ribosome-DARPin complexes was incubated for 1 h at 4 °C with 100 nM bEpEx in solution. The complexes bound to EpCAM were captured by incubating with 100 µl streptavidin-coated paramagnetic beads (Dynabeads MyOne Streptavidin) for 30 min at 4 °C. After washing the beads with WBT [50 mM Tris-acetate (pH 7.6), 150 mM NaCl, 50 mM Mg(CH₃COO⁻)₂ and 0.01% Tween-20], we eluted the mRNA with elution buffer [50 mM Tris-acetate (pH 7.6), 150 mM NaCl and 250 mM ethylenediaminetetraacetic acid (EDTA)] and prepared it for another round of selection. To minimize selection of unspecific binders, we pre-treated all tubes with TBST [50 mM Tris-acetate (pH 7.6), 150 mM NaCl and 0.05% Tween-20] supplemented with 0.1% of BSA. To further avoid binders against the streptavidin present on the paramagnetic beads, before each panning step, we preincubated the translation mix with the beads for 1 h at 4 °C and transferred the supernatant to a fresh tube.

Optimization by ribosome display

Selection of second-generation binders was performed as described^{8,9} with few modifications. First, EpCAM-specific DARPins selected by phage display or ribosome display were randomly mutated by error-prone PCR. Each DARPin was amplified individually in the presence of 3, 9 and 20 µM dNTP analogues dPTP [6-(deoxy-β-D-erythro-pentofuranosyl)-3,4-dihydro-8H-pyrimido-[4,5-c][1,2]oxazine-7-one-5'-triphosphate] and 8-oxo-dGTP (8-oxo-2'-deoxyguanosine-5'-triphosphate). Each amplification was performed in a 50-µl reaction in the presence of 1 µM primers, 1 unit of PlatinumTaq DNA Polymerase (Invitrogen), 5% dimethyl sulfoxide, 1.5 mM MgCl₂ and 200 µM dNTPs. PCR products were then pooled in equimolar amounts for selection experiments.

Four rounds of ribosome display were performed. In rounds 1 and 3, the translation mix was incubated for 1 h at 4 °C with 0.7 µM bEpEx, and subsequently, a 5000-fold excess of non-biotinylated EpEx was added to select for binders with a slow off-rate.²⁶ This mixture was kept

under slow shaking at 4 °C for 2 or 10 h, respectively. In rounds 2 and 4, 100 nM bEpEx were used in the panning step, and no non-biotinylated competitor was added to enrich correct clones without further selection pressure. mRNAs of complexes bound to bEpEx were isolated as described above.

Purification of DARPinS

Selected DARPinS from phage display and ribosome display were cloned into a pQE30-derived vector (Qiagen), containing an N-terminal MRGS(H)₆ tag and a C-terminal double stop codon (pQE30ss), or into pQE30-sfGFP, the latter to create DARPinS with a C-terminal fusion of sfGFP.²² For ELISAs, affinity measurements, labeling and flow cytometry, DARPinS were produced in soluble form in *E. coli* XL1-blue (Stratagene, La Jolla, USA) and purified using Ni-NTA Superflow (Qiagen) in gravity-flow columns as described.¹ For SPR and CD measurements, the proteins were further purified by preparative size-exclusion chromatography.

Size-exclusion chromatography

DARPinS (15 µM) in 50 µl PBS were analyzed on a Superdex-200 PC 3.2/30 column using either an ETTAN or an ÄKTA micro chromatography system (all GE Healthcare) at a flow rate of 60 µl/min and with PBS as running buffer. For preparative size-exclusion chromatography, DARPinS were purified on a Superdex-200 10/300 GL column using an ÄKTA explorer chromatography system (GE Healthcare) at a flow rate of 1 ml/min.

ELISA

MaxiSorp plates were coated with 100 µl of 66 nM neutravidin in PBS overnight at 4 °C. After washing, all wells were blocked with 300 µl PBS containing 0.2% of BSA for 1 h at room temperature. Protein targets were biotinylated and added to the wells to a final concentration of 50 nM (10 nM in competition ELISAs). Crude bacterial extract (100 µl, for screening of single clones from phage display and ribosome display selections) or purified DARPinS (100 µl, 200 nM for specificity and 10 nM in competition ELISAs) were added at room temperature. After 1 h, bound DARPinS were detected with an anti RGS-His₆ antibody conjugated with horseradish peroxidase (Qiagen) or with an anti-RGS-His₆ antibody (Qiagen) and an anti-mouse-IgG conjugated to alkaline phosphatase (Pierce). For the competition ELISA, the same setup as described above was used except that purified DARPinS were incubated with 100 nM non-biotinylated EpEx prior to incubation with immobilized EpCAM for 10 min at room temperature. For self-binding experiments, 100 nM DARPinS *in vivo*, biotinylated at an N-terminal Avi-tag, and 100 nM DARPinS with a C-terminal HA tag were mixed and incubated overnight at 4 °C. This DARPin mixture (100 µl) was then allowed to bind to neutravidin-coated wells for 1 h at 4 °C. After washing, complexes were detected with an anti-HA antibody conjugated with horseradish peroxidase (Sigma).

CD spectroscopy

CD spectra of DARPinS in PBS, pH 7.4, were recorded at 20, 96 and 20 °C after heating to 96 °C. Thermal denaturation was tracked at 222 nm every 0.5 °C by gradually heating the cuvette at 1 °C/min from 20 °C to 96 °C. The CD signal was converted to mean residue ellipticity using the concentration of the sample determined spectrophotometrically at 280 nm. Measurements were performed on a J-810 CD spectrometer (Jasco, Japan).

Labeling of DARPinS with Alexa Fluor 488

EpCAM-specific DARPinS as well as control DARPinS were cloned into a pQE30-based vector, appending two glycines and a unique cysteine at their C-terminus. These DARPinS were expressed and purified as described above. Cys-DARPinS (500 µM) were fully reduced by incubation with 50 mM tris-(2-carboxyethyl)phosphine for 30 min at 37 °C in PBS, pH 7.4. Tris-(2-carboxyethyl)phosphine removal and buffer exchange to degassed PBS, pH 7.1, were achieved with a HiTrap desalting column (GE Healthcare). Alexa Fluor 488 C₅-maleimide (Invitrogen) was added in 2-fold excess and incubated at 25 °C for 2 h. After quenching of unreacted dye with 10 mM dithiothreitol for 20 min at 25 °C, a PD-10 column (GE Healthcare) was used to remove unreacted dye and exchange the buffer to 100 mM sodium bicarbonate with 20 mM NaCl, pH 8. Monolabeled DARPin was separated from unlabeled protein by anion-exchange chromatography on a MonoQ 5/50 GL column using an ÄKTA explorer (both GE Healthcare) using 100 mM sodium bicarbonate with 1 M NaCl at pH 8 for isocratic elution.

Flow cytometry analysis

Flow cytometry analysis was performed to confirm the binding of DARPinS to EpCAM expressed on the surface of tumor cells. 1×10^6 cells were harvested and washed twice with PBS, then resuspended in FACS buffer (PBS and 1% BSA) containing the DARPin (fused to sfGFP, coupled to Alexa Fluor 488 or unlabeled) (100 nM) and incubated for 45 min on ice. Unlabeled DARPinS were detected using anti-RGS-His antibody (Qiagen) and a goat anti-mouse FITC-labeled secondary antibody (Invitrogen). Cells were washed three times between all incubation steps with FACS buffer. After the final wash, cells were resuspended in 1 ml FACS buffer and subjected to flow cytometry using a FACSCalibur or FACSCanto II flow cytometer (both BD Bioscience). For each experiment, 1×10^4 cells were counted. Data were analyzed using the FlowJo software (Tree Star, Ashland/Oregon, USA).

For competition experiments with unlabeled DARPinS, 5×10^5 HT29 cells were incubated with 100 nM Ec4-sfGFP or Ac2-sfGFP fusion proteins or the monoclonal anti-EpCAM antibody MOC31 for 30 min on ice. For competition, the cells were preincubated with 10 µM DARPinS Ec4 or Ac2 for 15 min on ice. MOC31-treated samples were additionally incubated with 2 µg/ml Alexa Fluor 488-coupled goat anti-mouse IgG (Invitrogen) for 20 min on ice. Cells were then analyzed by flow cytometry as described above.

Affinity determination

Affinity determination on cells

Harvested MCF-7 cells were preincubated for 30 min at 37 °C in FACS buffer supplemented with 0.2% sodium azide to inhibit internalization. For equilibrium experiments, 3×10^5 cells in 500 μ l were incubated for 1 h at 4 °C with different concentrations of DARPin fused to sfGFP or coupled to Alexa Fluor 488 ranging from 100 pM to 1 μ M. After one washing step, MFIs were measured on a FACSCanto II flow cytometer (BD Bioscience). Values for nonspecific binding were obtained by incubating the cells for 60 min at 4 °C with 5 μ M unlabeled tetravalent Ec1-LZ-Ac2 prior to a washing step and the addition of fluorescent DARPins. For dissociation rate experiments, 3×10^5 cells were saturated for 1 h at 4 °C with 100 nM DARPin fused to sfGFP or coupled to Alexa Fluor 488. Thereafter, cells were washed and resuspended with 1 μ M DARPin as an unlabeled competitor to prevent rebinding. MFIs were recorded at different time points between 0 and 4 h. For association rate experiments, 3×10^5 cells were incubated with 2.5, 7.5 or 22.5 nM DARPin fused to sfGFP or coupled to Alexa Fluor 488 and measured at times between 1 and 60 min without prior washing. Background association of an unselected DARPin library member, E3_5 fused to sfGFP, was subtracted. For indirect off-rate measurements, 6×10^5 cells in 1 ml were saturated for 1 h at 4 °C with 200 nM unlabeled DARPin to be tested, then centrifuged and resuspended with Ec4-, Ec1- or Ac2-sfGFP (2 μ M). Association of the labeled monovalent binder was measured at different time points between 0 and 4 h. This high concentration of monovalent binder leads to instantaneous binding on cells with free EpCAM, but on cells previously saturated with unlabeled test DARPin, it occurred at the rate of dissociation of the unlabeled DARPin. Data evaluation was performed with Prism (GraphPad).

Affinity determination by SPR

The EpCAM-binding affinity of the DARPins was measured by SPR using a ProteOn XPR36 (Bio-Rad Laboratories, Hercules, USA) or a Biacore 3000 (GE Healthcare) instrument. For ProteOn measurements, one ligand channel of a Neutravidin (NLC) Sensor Chip was coated with 300 resonance units of the extracellular domain of EpCAM (residues 1–242 of the mature protein) biotinylated using an AviTag. Kinetic data were obtained by parallel injection of different concentrations of DARPins ranging from 0.32 to 31.6 nM at a buffer flow rate of 60 μ l/min in PBS, pH 7.4, containing 3 mM EDTA and 0.005% Tween-20. Data evaluation was performed using the ProteOn Manager software (Bio-Rad Laboratories). For Biacore measurements, a streptavidin (SA) chip was coated with 120 resonance units of biotinylated extracellular domain of EpCAM. Binding kinetics were determined by serial injection of different concentrations of DARPins ranging from 10 to 160 nM at a buffer flow rate of 30 μ l/min in HBST [20 mM Hepes (pH 7.4), 150 mM NaCl, 3 mM EDTA and 0.005% Tween-20]. Data were evaluated using the BIAEVAL software (GE Healthcare) and Scrubber 2 (BioLogic Software, Campbell, Australia).

Multivalent constructs

A leucine zipper domain (RMKQLEDKVEELLSKNYH-LENEVARLKKLVGER) derived from GCN4 flanked by short linkers (GGGG and GGSS) was inserted into pQE30ss (see above). Bivalent and tetravalent constructs were generated by fusing DARPins to either or both ends of the dimerization domain (Fig. 7a). Multivalent DARPins were expressed and purified as described above.

Determination of internalization by confocal microscopy

MCF-7 cells (2×10^5 cells) were seeded on coverslips and incubated for 24 h at 37 °C and 5% CO₂. For competition, cells were preincubated with unlabeled EpCAM binders, Ec4 and Ac2, at a final concentration of 5 μ M (diluted in DMEM) for 15 min at 37 °C. Then, EpCAM-specific DARPins, Eph1, Ec4 and Ac2, and the unspecific DARPin off7 labeled at an engineered C-terminal cysteine (see above) with Alexa Fluor 488 were added to the cells at a final concentration of 100 nM (diluted in DMEM). After 1 h of incubation at 37 °C or at 4 °C with the labeled DARPins, the cells were washed three times with PBS for 5 min each time and fixed with 4% paraformaldehyde in PBS (10 min at room temperature). Thereafter, the cells were rinsed with PBS, and the nuclei were stained with 0.8 μ g/ml 4',6-diamidino-2-phenylindole in PBS for 2 min. The coverslips were then quickly washed with PBS, mounted on glass slides with Fluoromount G (Southern Biotech) and sealed with nail polish. The glass slides were kept in the dark at 4 °C until confocal microscopy was done. Fluorescent images were recorded using a confocal laser scanning microscope (TCS-SP 2; Leica, Mannheim, Germany) with a selected confocal plane approximately in the middle of the cell. Images were processed using Imaris 3D software (Bitplane).

In vitro cytotoxicity of DARPin-based fusion toxins

The cytotoxicity of the various EpCAM-specific ETA" fusion toxins and the irrelevant control fusion toxin E3_5-ETA" was tested on EpCAM-positive HT29 colon carcinoma cells as described,¹⁶ using a standard colorimetric XTT cell proliferation kit II (Roche) upon 72 h of exposure. The expression and purification of the toxin fusions has been carried out as described before.¹⁶

Supplementary materials related to this article can be found online at [doi:10.1016/j.jmb.2011.09.016](https://doi.org/10.1016/j.jmb.2011.09.016)

Acknowledgements

The authors thank Dr. Daniel Steiner and Petra Parizek for their support with phage display and ribosome display selections and Manuel Simon and Dr. Ykelien Boersma for helpful discussions. This work was supported by Swiss National Science Foundation grants 310030–119859 (to U.Z.W.) and 3100A0–12867/1 (to A.P.) and the Krebsliga of the Kanton Zürich.

References

1. Binz, H. K., Stumpp, M. T., Forrer, P., Amstutz, P. & Plückthun, A. (2003). Designing repeat proteins: well-expressed, soluble and stable proteins from combinatorial libraries of consensus ankyrin repeat proteins. *J. Mol. Biol.* **332**, 489–503.
2. Binz, H. K., Amstutz, P., Kohl, A., Stumpp, M. T., Briand, C., Forrer, P. *et al.* (2004). High-affinity binders selected from designed ankyrin repeat protein libraries. *Nat. Biotechnol.* **22**, 575–582.
3. Zahnd, C., Pecorari, F., Straumann, N., Wyler, E. & Plückthun, A. (2006). Selection and characterization of Her2 binding-designed ankyrin repeat proteins. *J. Biol. Chem.* **281**, 35167–35175.
4. Boersma, Y. L. & Plückthun, A. (2011). DARPins and other repeat protein scaffolds: advances in engineering and applications. *Curr. Opin. Biotechnol.* doi:10.1016/j.copbio.2011.06.004.
5. Interlandi, G., Wetzel, S. K., Settanni, G., Plückthun, A. & Caflisch, A. (2008). Characterization and further stabilization of designed ankyrin repeat proteins by combining molecular dynamics simulations and experiments. *J. Mol. Biol.* **375**, 837–854.
6. Kramer, M. A., Wetzel, S. K., Plückthun, A., Mittl, P. R. & Grütter, M. G. (2010). Structural determinants for improved stability of designed ankyrin repeat proteins with a redesigned C-capping module. *J. Mol. Biol.* **404**, 381–391.
7. Hanes, J. & Plückthun, A. (1997). *In vitro* selection and evolution of functional proteins by using ribosome display. *Proc. Natl Acad. Sci. USA*, **94**, 4937–4942.
8. Zahnd, C., Amstutz, P. & Plückthun, A. (2007). Ribosome display: selecting and evolving proteins *in vitro* that specifically bind to a target. *Nat. Methods*, **4**, 269–279.
9. Zahnd, C., Wyler, E., Schwenk, J. M., Steiner, D., Lawrence, M. C., McKern, N. M. *et al.* (2007). A designed ankyrin repeat protein evolved to picomolar affinity to Her2. *J. Mol. Biol.* **369**, 1015–1028.
10. Steiner, D., Forrer, P., Stumpp, M. T. & Plückthun, A. (2006). Signal sequences directing cotranslational translocation expand the range of proteins amenable to phage display. *Nat. Biotechnol.* **24**, 823–831.
11. Steiner, D., Forrer, P. & Plückthun, A. (2008). Efficient selection of DARPins with sub-nanomolar affinities using SRP phage display. *J. Mol. Biol.* **382**, 1211–1227.
12. Zahnd, C., Kawe, M., Stumpp, M. T., de Pasquale, C., Tamaskovic, R., Nagy-Davidescu, G. *et al.* (2010). Efficient tumor targeting with high-affinity designed ankyrin repeat proteins: effects of affinity and molecular size. *Cancer Res.* **70**, 1595–1605.
13. Went, P. T., Lugli, A., Meier, S., Bundi, M., Mirlacher, M., Sauter, G. & Dirnhofer, S. (2004). Frequent EpCAM protein expression in human carcinomas. *Hum. Pathol.* **35**, 122–128.
14. Münz, M., Baeuerle, P. A. & Gires, O. (2009). The emerging role of EpCAM in cancer and stem cell signaling. *Cancer Res.* **69**, 5627–5629.
15. Winkler, J., Martin-Killias, P., Plückthun, A. & Zangemeister-Wittke, U. (2009). EpCAM-targeted delivery of nanocomplexed siRNA to tumor cells with designed ankyrin repeat proteins. *Mol. Cancer Ther.* **8**, 2674–2683.
16. Martin-Killias, P., Stefan, N., Rothschild, S., Plückthun, A. & Zangemeister-Wittke, U. (2011). A novel fusion toxin derived from an EpCAM-specific designed ankyrin repeat protein has potent antitumor activity. *Clin. Cancer Res.* **17**, 100–110.
17. Balzar, M., Winter, M. J., de Boer, C. J. & Litvinov, S. V. (1999). The biology of the 17-1A antigen (Ep-CAM). *J. Mol. Med.* **77**, 699–712.
18. Münz, M., Kieu, C., Mack, B., Schmitt, B., Zeidler, R. & Gires, O. (2004). The carcinoma-associated antigen EpCAM upregulates *c-myc* and induces cell proliferation. *Oncogene*, **23**, 5748–5758.
19. Maetzel, D., Denzel, S., Mack, B., Canis, M., Went, P., Benk, M. *et al.* (2009). Nuclear signalling by tumour-associated antigen EpCAM. *Nat. Cell Biol.* **11**, 162–171.
20. Dreier, B. & Plückthun, A. (2011). Ribosome display: a technology for selecting and evolving proteins from large libraries. *Methods Mol. Biol.* **687**, 283–306.
21. Ditzel, H. J. (2002). Rescue of a broader range of antibody specificities using an epitope-masking strategy. *Methods Mol. Biol.* **178**, 179–186.
22. Pedelacq, J. D., Cabantous, S., Tran, T., Terwilliger, T. C. & Waldo, G. S. (2006). Engineering and characterization of a superfolder green fluorescent protein. *Nat. Biotechnol.* **24**, 79–88.
23. Griep, R. A., van Twisk, C., van der Wolf, J. M. & Schots, A. (1999). Fluobodies: green fluorescent single-chain Fv fusion proteins. *J. Immunol. Methods*, **230**, 121–130.
24. Balzar, M., Briare-de Bruijn, I. H., Rees-Bakker, H. A., Prins, F. A., Helfrich, W., de Leij, L. *et al.* (2001). Epidermal growth factor-like repeats mediate lateral and reciprocal interactions of Ep-CAM molecules in homophilic adhesions. *Mol. Cell. Biol.* **21**, 2570–2580.
25. Zaccolo, M., Williams, D. M., Brown, D. M. & Gherardi, E. (1996). An approach to random mutagenesis of DNA using mixtures of triphosphate derivatives of nucleoside analogues. *J. Mol. Biol.* **255**, 589–603.
26. Zahnd, C., Sarkar, C. A. & Plückthun, A. (2010). Computational analysis of off-rate selection experiments to optimize affinity maturation by directed evolution. *Protein Eng. Des. Sel.* **23**, 175–184.
27. Merz, T., Wetzel, S. K., Firbank, S., Plückthun, A., Grütter, M. G. & Mittl, P. R. (2008). Stabilizing ionic interactions in a full-consensus ankyrin repeat protein. *J. Mol. Biol.* **376**, 232–240.
28. Kaufmann, K. W., Lemmon, G. H., Deluca, S. L., Sheehan, J. H. & Meiler, J. (2010). Practically useful: what the Rosetta protein modeling suite can do for you. *Biochemistry*, **49**, 2987–2998.
29. Tamaskovic, R., Simon, M., Stefan, N., Schwill, M. & Plückthun, A. (in press). Designed Ankyrin Repeat Proteins (DARPins): From research to therapy. *Methods Enzymol.*
30. Hussain, S., Plückthun, A., Allen, T. M. & Zangemeister-Wittke, U. (2006). Chemosensitization of carcinoma cells using epithelial cell adhesion molecule-targeted liposomal antisense against bcl-2/bcl-xL. *Mol. Cancer Ther.* **5**, 3170–3180.
31. Hussain, S., Plückthun, A., Allen, T. M. & Zangemeister-Wittke, U. (2007). Antitumor activity of an epithelial cell adhesion molecule targeted

- nanovesicular drug delivery system. *Mol. Cancer Ther.* **6**, 3019–3027.
32. Di Paolo, C., Willuda, J., Kubetzko, S., Lauffer, I., Tschudi, D., Waibel, R. *et al.* (2003). A recombinant immunotoxin derived from a humanized epithelial cell adhesion molecule-specific single-chain antibody fragment has potent and selective antitumor activity. *Clin. Cancer Res.* **9**, 2837–2848.
33. Morfill, J., Blank, K., Zahnd, C., Luginbühl, B., Kühner, F., Gottschalk, K. E. *et al.* (2007). Affinity-matured recombinant antibody fragments analyzed by Single molecule force spectroscopy. *Biophys. J.* **93**, 3583–3590.